Cells and Materials

Volume 2 | Number 4 Article 7

1992

Apatite - Cholesterol Agglomerates in Human Atherosclerotic Lesions

Sara Sarig
The Hebrew University of Jerusalem

Danielle Hirsch
The Hebrew University of Jerusalem

Reuven Azoury
The Hebrew University of Jerusalem

Teddy A. Weiss
The Hebrew University of Jerusalem

Iony Katz
Hadassah Hosptial, Jerusalem

See next page for additional authors

Follow this and additional works at: https://digitalcommons.usu.edu/cellsandmaterials

 Part of the Biomedical Engineering and Bioengineering Commons

Recommended Citation

Sarig, Sara; Hirsch, Danielle; Azoury, Reuven; Weiss, Teddy A.; Katz, Iony; and Kruth, Howard S. (1992) "Apatite - Cholesterol Agglomerates in Human Atherosclerotic Lesions," *Cells and Materials*: Vol. 2 : No. 4 , Article 7.
Available at: https://digitalcommons.usu.edu/cellsandmaterials/vol2/iss4/7

This Article is brought to you for free and open access by the Western Dairy Center at DigitalCommons@USU. It has been accepted for inclusion in Cells and Materials by an authorized administrator of DigitalCommons@USU. For more information, please contact digitalcommons@usu.edu.

Apatite - Cholesterol Agglomerates in Human Atherosclerotic Lesions

Authors

Sara Sarig, Danielle Hirsch, Reuven Azoury, Teddy A. Weiss, Iony Katz, and Howard S. Kruth

This article is available in Cells and Materials: https://digitalcommons.usu.edu/cellsandmaterials/vol2/iss4/7

CELLS AND MATERIALS, Vol. 2, No. 4, 1992 (Pages 339-346) 1051-6794/92$3.00+.00
Scanning Microscopy International, Chicago (AMF O'Hare), IL 60666 USA

APATITE - CHOLESTEROL AGGLOMERATES IN HUMAN ATHEROSCLEROTIC LESIONS

Sara Sarig[1], Danielle Hirsch[1], Reuven Azoury[1], Teddy A. Weiss[2], Iony Katz[2], and Howard S. Kruth[3,*]

[1]Casali Institute of Applied Chemistry, Graduate School of Applied Science and Technology, The Hebrew University of Jerusalem, 91904 Jerusalem, Israel
[2]Department of Cardiology, Hadassah Hospital, Jerusalem, Israel
[3]Section of Experimental Atherosclerosis, National Heart, Lung, and Blood Institute, National Institutes of Health, Bethesda, MD 20892, USA

(Received for publication October 19, 1992, and in revised form December 11, 1992)

Abstract

The purpose of this study was to examine the ultrastructural relationships of cholesterol crystals and apatite deposits in human atherosclerotic lesions. Segments of human aortic atherosclerotic lesions were obtained at autopsy, fixed in glutaraldehyde and dehydrated without using any organic solvents. The aortic segments were coated with carbon and subjected to various scanning electron microscope analyses. These included secondary electron imaging, back scattering of primary electrons, energy dispersive X-ray analysis of selected spots followed by area mapping of calcium and phosphorus, and cathodoluminescence.

The information gathered from scanning of selected areas in the lesions by all the techniques showed that cholesterol crystals and apatite deposits are close to each other, within 10 μm distance or less. Cholesterol crystals are often surrounded by or adjacent to apatite.

The results indicate that cholesterol and apatite crystals form closely linked agglomerates in human atherosclerotic lesions. Further studies are needed to determine whether precipitation of calcium and cholesterol are somehow linked during atherosclerotic lesion development.

Key Words: Calcium phosphate, apatite, cholesterol, atherosclerotic lesion, scanning electron microscopy, secondary electron imaging, back scattering electron imaging, energy dispersive X-ray analysis, cathodoluminescence.

*Address for correspondence:
Howard S. Kruth
National Institutes of Health
Building 10, Room 5N-113
Bethesda, MD 20892

Telephone: 301-496-4827

Introduction

The pathogenesis of atherosclerotic lesions is multifactorial. There are many physiological and metabolic reasons to reach this conclusion, not the least being the complexity of the composition and ultrastructure of the lesions. Attempts have been made to unify the roles of connective tissue proteins and proteoglycans in the accumulation of lipids, lipoproteins and calcium in atherosclerotic plaques (Hollander, 1976).

Arterial calcification has been described occurring both as a primary and a secondary phenomenon. Primary calcification develops in seemingly unchanged arterial walls, often showing regular patterns, whereas secondary calcification, which appears in atherosclerotic lesions, is irregularly distributed along the thickened atherosclerotic intima (Meyer *et al.*, 1977). Recently, attention has been drawn to the fact that degeneration of smooth muscle cells may be involved in calcification (Tanimura *et al.*, 1986).

After it had been discovered that a polyene antibiotic compound, filipin, interacts directly with unesterified cholesterol (Norman *et al.*, 1972; Bittman and Fischkoff, 1972), and that their complex had a unique molecular structure (deKruijff and Demel, 1974), a staining technique was introduced to identify unesterified cholesterol in human atherosclerotic lesions. Using this technique, Kruth (1984) was able to differentiate between esterified cholesterol, which is easily stained by oil red 0, and unesterified cholesterol which is not stained by this dye, but which can be stained with the fluorescence probe, filipin. He found that esterified and unesterified cholesterol were located in separate regions in the lesions. In addition, he observed that unesterified cholesterol often was co-localized with calcium deposits. However, little data has been obtained concerning the ultrastructural relationships of calcium and cholesterol in lesions. The ideal instrument for such investigations is the scanning electron microscope (SEM) (Boyde *et al.*, 1986).

Sims (1989) reviewed an extensive list of SEM studies carried out on the arteries of experimental animals, remarking that surprisingly few applications of this technique in research on human arteries had been

reported until that time. An extensive chemical and physicochemical study on the mineral deposits of human atherosclerotic aorta confirmed that apatite was the major component of the mineral phase (Schmid *et al.*, 1980). The mineral deposits prepared for SEM were exhaustively delipidated using a mixture of chloroform and ethanol. The deposits were heterogeneous with regard to shape. Of course, no interconnection with cholesterol could be observed, as all the lipids were dissolved and washed away by the sample preparation procedure. No cholesterol deposits have been identified in other SEM studies of calcified atherosclerotic deposits (Matonoha and Zechmeister, 1978; Tomazic *et al.*, 1988) in which the specimens were dehydrated in alcohol and the organic constituents were removed by hydrazine treatment.

In the present study, sections of human lesions obtained at autopsy were fixed in glutaraldehyde, dehydrated (without using any organic solvent) by lyophilization, and subjected to SEM analyses. These analyses included viewing the structure by secondary electrons (SE imaging) to visualize general structure, using back scattered electron imaging (BSEI) to outline the areas in which heavy elements (in this case, Ca and P) were present, and energy dispersive X-ray analysis (EDX) for the identification and localization of calcium phosphate.

In addition to these well established techniques, we have identified cholesterol crystals using cathodoluminescence (CL) (Giles, 1975). Biological materials show inherent CL emission that makes it possible to obtain CL micrographs. Not all organic compounds possess equal CL potential. Among the organic molecules, an especially high CL emission is obtained from π-electrons in unsaturated six and five membered ring compounds (Pease and Hayes, 1966) such as cholesterol. A CL image of the specimen may be obtained in SEM through continuous monitoring of the emitted light (Giles, 1975).

The above techniques, including the newly introduced CL mode for cholesterol identification, allowed us to obtain an integrated view of calcium and cholesterol in a defined segment of a lesion. This approach is useful in examining important features of human atherosclerotic lesion ultrastructure.

Experimental

Aortas were obtained at autopsy from three patients (54-years-old female, 45-years-old male, and 64-years-old male) who died from myocardial infarction. The aortas were opened by a longitudinal incision. Segments with either fatty deposits or ulceration were cut out with a scalpel. All lesions studied were advanced atherosclerotic plaques. Some of the segments were hard and non-elastic, indicating the presence of mineral deposits. Tissue was stored in 2% glutaraldehyde at 4°C.

In the first stage of processing, the segments were rapidly frozen as described below. A cryostat was filled with liquid nitrogen and a Freon trap tube was installed inside it. The segments were first immersed in the Freon trap and then the segments were immediately transferred into the liquid nitrogen. In the second stage of processing, the segments were lyophilized at -50°C and 25 microns Hg pressure for 3 hours.

The lyophilized segments were fixed on SEM stubs with carbon paint. Some of them were positioned to view ulcerated lesions from the luminal surface (i.e., the lumen faced the electron beam) and some were positioned to view a cross-section of the arterial wall. The specimens were coated with carbon and kept under vacuum until SEM analysis.

The SEM analysis, on a JEOL 840 SEM, included five techniques. The first was secondary electron imaging (SEI) to visualize overall structures. The second was back scattered electrons imaging (BSEI) from the same site as the SEI. These BSEI images provided a means to identify areas in which relatively heavy elements were concentrated. The third technique was energy dispersive X-ray analysis (EDX) linked with SEM. This technique made possible identification of elements heavier than fluorine which were present in those areas delineated by BSEI. Calcium and phosphorus were identified by comparing the peak energy levels obtained from samples with those of calcium and phosphorus in apatite produced and characterized as described previously (Lerner *et al.*, 1989). The ratio of the calcium to phosphorus intensity levels was estimated, thus providing an indication of the nature of the mineral phase of calcium phosphate present. We studied only those mineral deposits with a 5:3 calcium to phosphorus molar ratio, characteristic of apatite. The fourth technique consisted of mapping the density of the identified elements to delineate the limits of the mineral regions. The sample area was scanned about 120 times. The regions where the determined element was present were marked by dots. The black and white density maps were transformed by image processing into color density maps in which colors corresponded to the relative density of dots. The relative density of dots depended on the concentration of the mineral phase. The maps of elements were displayed on a computer console screen and photographed by a computer controlled camera. The fifth method consisted of cathodoluminescence (CL) imaging. CL scanning was carried out at sites at which SEI and BSEI had been performed. CL results from low energy photons, corresponding to visible light. The CL signal was collected by a light guide and amplified with a photomultiplier.

Results and Discussion

The main difference between previous SEM studies of calcification in blood vessels (Matonoha and Zechmeister, 1978; Tomazic *et al.*, 1988) and the present work was the methodology for preparing samples. Water and organic molecules were removed from atherosclerotic lesions in previous studies using alcohols or mixtures of alcohols and other organic solvents. These

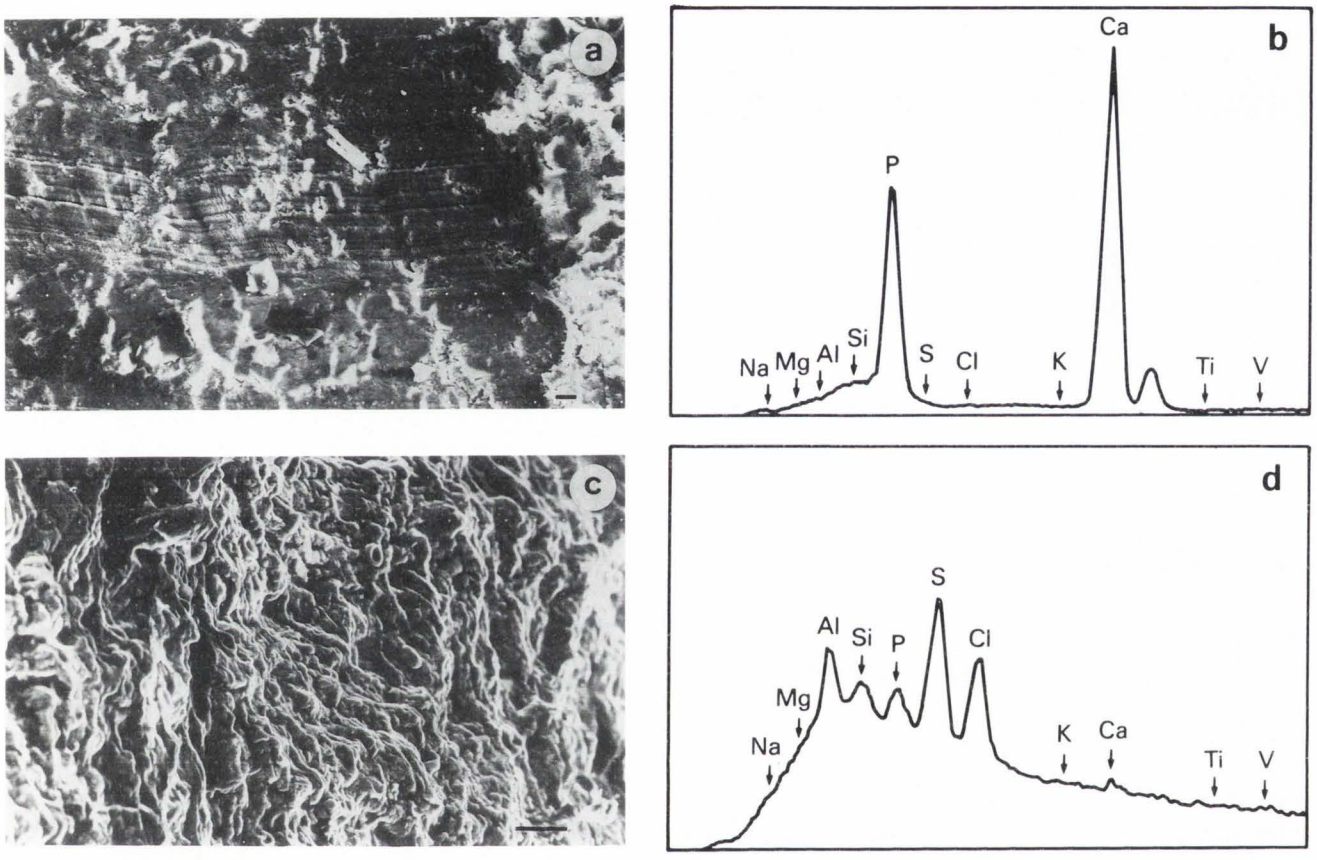

Figure 1. (**a**) A cross-section of a hardened part of an atherosclerotic lesion shown by SEI; bar = 10 μm. (**b**) EDX spectrum obtained from the same field as shown in a. Only peaks of Ca and P were detected; the Ca:P ratio is about 5:3. (**c**) A cross-section of a soft part of an atherosclerotic lesion shown by SEI; bar = 10 μm. (**d**) EDX spectrum obtained from the same field as shown in c. No significant Ca peak is present; peaks of Al, Cl, S and a small peak of P, apparently from phospholipids are evident.

solvents also unavoidably dissolve the unesterified cholesterol crystals present in the lesions. In the present study, the aorta segments were frozen in liquid nitrogen and afterward lyophilized thus preserving the cholesterol crystals.

The ultrastructure of lesions consists of regions with different features. In Fig. 1a, the SEI photomicrograph shows a layered structure about 350 μm long within a hard lesion. This same area was examined by EDX. The response was uniform throughout the area, with only calcium and phosphorus detectable at about a 5:3 molar ratio indicating that this area was composed of apatite. Fig. 1b shows an EDX spectrum collected for 52 seconds at a random spot demonstrating the calcium and phosphorus peaks. In Fig. 1c, a different appearing region of a soft lesion is shown by SEI. The EDX scan (Fig. 1d) of this region did not show any significant calcium peak, indicating that no significant calcification existed in this region. The time of exposure for the analysis of this spot was 126 seconds and the sensitivity was higher than that used to produce the spectrum in Fig. 1b. Thus, the background noise is increased. With this configuration, the significant peaks were: chlorine (remnants from the saline solution), aluminum (from the sample bearing stub), and sulfur, the most pronounced peak, which may be attributed to sulfur containing proteins. The smaller phosphorus peak may be possibly due to phospholipids or phosphoproteins. It follows that the wavy material in Fig. 1c is most probably due to an organic material.

Most randomly scanned areas of the lesions were not as homogeneous as the areas selected in Figs. 1a and 1c, but rather contained organic and mineral parts in close proximity. Crystalline deposits were distinguishable from organic tissue by morphological appearance. However, whereas some of the crystals were identified by EDX and BSEI as calcium phosphate, others did not yield any signal. These other crystals were presumably cholesterol. Our concern was to identify them as such by a positive response.

In order to show the specific response of cholesterol to CL in close vicinity to calcium phosphate, we prepared a sample of an agglomerate of cholesterol and apatite crystals, *in vitro*. The apatite crystals were precipitated by the method of Lerner *et al.* (1989), and afterward immersed in an ethanolic solution of cholesterol.

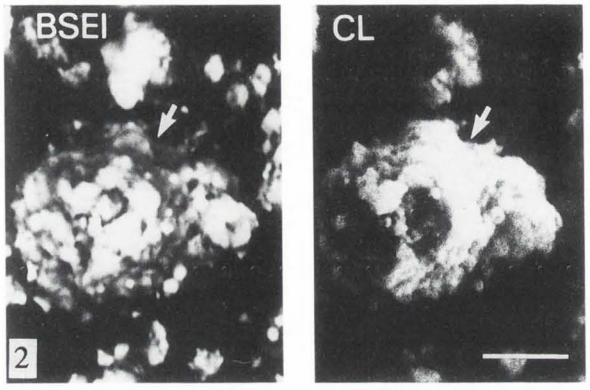

Figure 2. An apatite cholesterol crystal agglomerate produced *in vitro*. Left-hand photomicrograph shows BSEI. Right-hand photomicrograph shows CL image. The central apatite particle is partly covered by cholesterol and surrounded by small apatite crystallites. Arrows point to a region which is dark in BSEI and bright in CL image, indicating the presence of cholesterol. Bar = 10 μm.

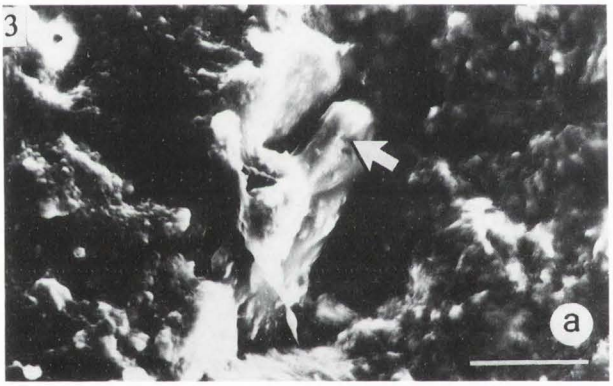

Figure 3. (**a**) A SEI photomicrograph of a segment of a hard atherosclerotic lesion viewed from the lesion. (**b**) A BSEI photomicrograph of the same region shown in a. Note the black gap in the center (arrow) indicating the absence of mineral components. (**c**) CL image of the same region shows an illuminated central plate. The arrow points towards the edge of the cholesterol plate embedded in the surrounding mineral component. Bar = 10 μm.

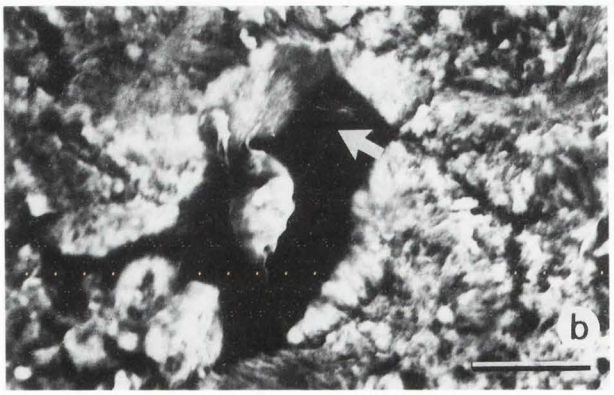

Figure 4. (**a**) SEI photomicrograph of a hard lesion segment viewed from the lumen. (**b**) BSEI of the same region as in a. Note the disappearance of the particle designated C and retention of particle designated A. (**c**) Map of calcium in a by scanning specific Ca energy level. Only a part of the ultrastructure shown in a contains calcium. The black areas contain organic matter. The zone scanned in c and d was slightly displaced from the zone shown in a and b. (**d**) Map of phosphorus in a by scanning specific P energy level. Note the identity of the phosphorus- and calcium-containing areas. This indicates the presence of a calcium phosphate compound. The relative concentrations of the elements were obtained on a screen as a pattern of dots. The denser the dot pattern, the higher the concentration of the element in a particular location. The dot density pattern was transformed into arbitrarily selected colors. The scale of the color transform is located at the bottom of Figure 5 and is divided into 15 degrees, the highest concentration represented by white. There is a remarkable correlation between the calcium and phosphorus maps with respect to dot density. The yellow-brown colored areas in the calcium map are well-matched with the blue areas in the phosphorus map. This would have been expected from an apatite deposit in which the Ca:P ratio was 5:3. Bars = 10 μm.

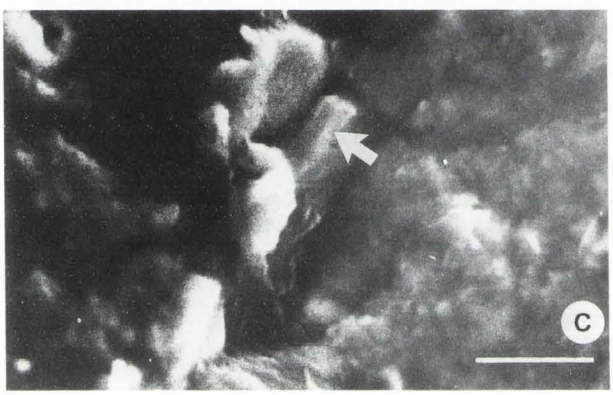

Figure 5. (**a**) SEI photomicrograph of a layered aggregate in a hard lesion segment viewed from the lumen. The arrow shows a protruding perpendicular plane. Bar = 10 μm. (**b**) A CL image of the same aggregate as in b, identifying it as a cholesterol crystal. Bar = 10 μm. (**c**) Map of calcium in the aggregate shown in a and b. The contour of the black area corresponds closely to that of the cholesterol crystal. (**d**) Map of phosphorus in the aggregate shown in a and b. The phosphorus area is identical to the calcium area. The color intensity of the phosphorus map is lower confirming the 5:3 Ca:P atom ratio in apatite. The magnification of c and d is slightly greater than that of a and b.

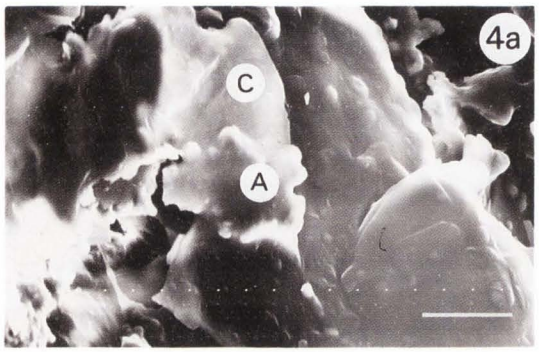
4a
C
A

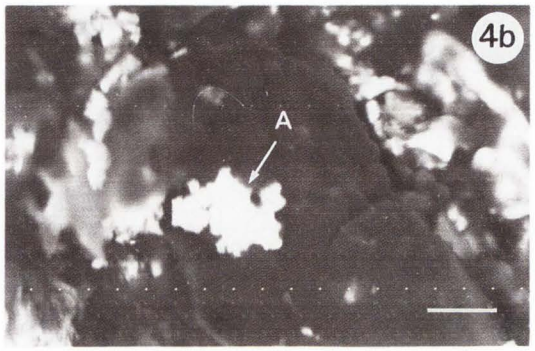
4b
A

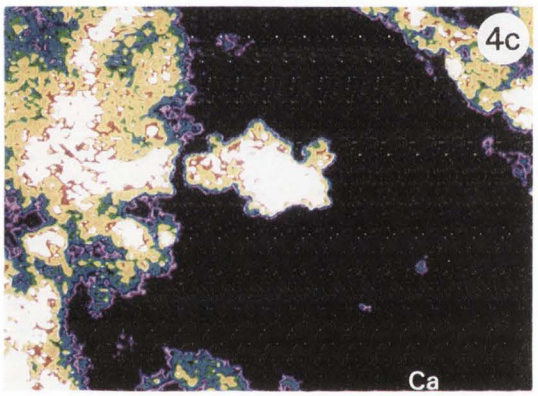
4c
Ca

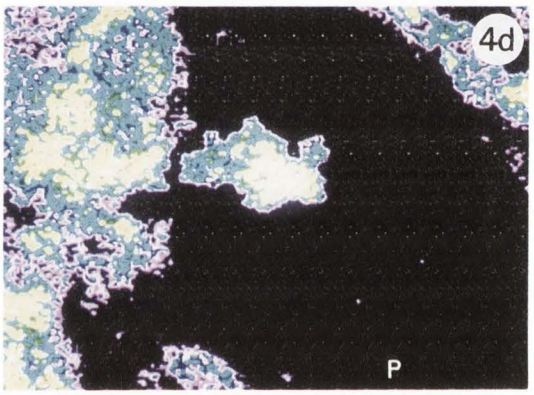
4d
P

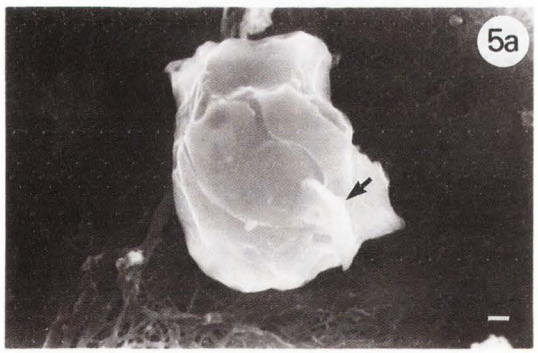
5a

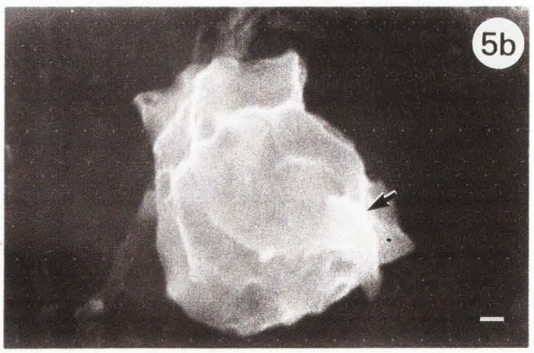
5b

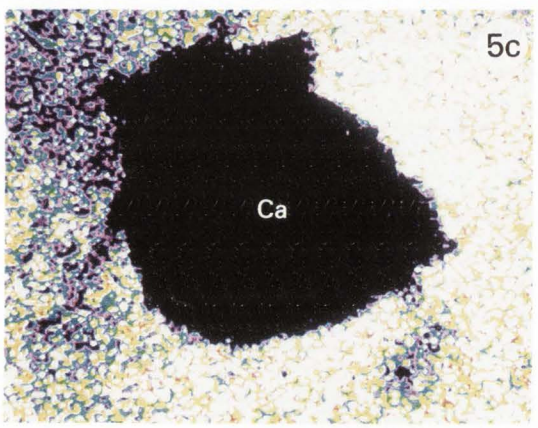
5c
Ca

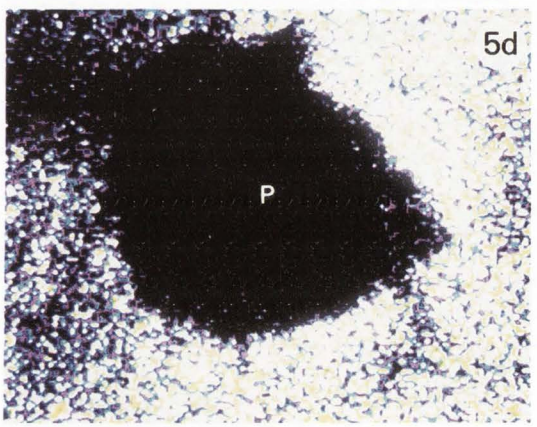
5d
P


COLOUR TRANSFORM
1 2 3 4 5 7 8 9 10 11 12 13 14 15

As shown in a previous study, deposition of cholesterol occurred upon the apatite crystals (Hirsch *et al.*, 1990).

Fig. 2 shows an agglomerate of apatite and cholesterol crystals viewed by BSEI (left photomicrograph) and by CL (right photomicrograph). In the BSEI photomicrograph there are many small particles surrounding the large central particle. The small satellite particles yield strong back scattering signals, indicating the presence of heavy elements. In this defined experimental system they can be only calcium and phosphorus. These small calcium phosphate particles yield a very faint CL signal, or no signal at all (see the right-hand photomicrograph).

The central large particle (about 20 μm long) is evidently an agglomerate of apatite crystallites in association with cholesterol crystallites. It can be seen that the areas emitting the strongest CL signals do not yield back scattering signals and vice versa. For instance, the upper part of this agglomerate is well visualized by CL (arrow) and quite dark in BSEI. Thus, a cholesterol crystal may be distinguished from the calcium phosphate background by its high intensity CL response, although the mineral itself has a certain degree of response to CL. The degree of CL response for mineral depends upon the view angle of the sample with respect to the detector.

Figs. 3-5 show SEM analysis of atherosclerotic lesion segments. However, in all cases when an analysis of BSEI or CL was carried out, the area was first examined by EDX to ascertain whether the area was organic or mineral. Fig. 3a shows a SEI photomicrograph of a zone of a lesion that contained both organic and mineral elements as determined by EDX analysis. Fig. 3b is the BSEI of the same zone. The background is very bright, indicating the presence of heavy elements (identified as calcium phosphate by EDX in data not shown). The arrow in (a) points to a tilted plate about 10 μm long and about 1.5 μm wide with a discernible right angle. This crystalline structure in (a) is absent in (b). The absence of this structure in the BSEI photomicrograph (b) means that the structure is organic. This organic crystalline structure shows cathodoluminescence in (c), indicating its identity as cholesterol.

A segment of an atherosclerotic plaque, taken from another donor, was analyzed and results are presented in Fig. 4. Fig. 4a displays a SEI photomicrograph showing two very close particles marked A and C. By SEI, these two particles do not appear particularly different from each other. As both particles appear on the same photomicrograph, the perpendicular distance between them cannot be larger than the focal distance, which, at the employed magnification is a maximum of 10 μm. Fig. 4b shows the same region by BSEI. In the BSEI photomicrograph the particle marked C completely disappeared from view, and most of the right part of the deposit became very faint. By contrast, the aggregate marked A is clearly visible in the BSEI photomicrograph. EDX analysis indicated that the aggregate marked A (which has a very distinctive shape) was apatite. Additionally, other parts, not clearly recognizable in the SEI picture (Fig. 4a), are evidently apatite (Fig. 4b).

The zone in (a) and (b) was scanned to localize the radiation specific to calcium (Fig. 4c) and phosphorus (Fig. 4d) energy levels. The regions showing the presence of phosphorus and calcium are exact replicas of each other, proving that the two elements are contained in the same places as might have been expected from the existence of a single compound, namely calcium phosphate. In the majority of the matching areas the concentration of phosphorus is lower than that of calcium. This would have been expected from an apatite deposit in which the Ca:P ratio is 5:3. The particle marked C in Fig. 4a as well as the whole contiguous structure to the right are evidently organic as shown by the lack of calcium or phosphorus signals in Figs. 4c and 4d.

The area scanned in Fig. 4 is about 60 μm x 40 μm. In a typical 4 mm x 4 mm sample of the lesion about 7-10 such areas containing calcium phosphate deposits could be found by SEM. In some locations the calcium phosphate deposits were aligned and in other locations deposits were unassociated with one another, separated by areas of organic tissue, in which crystalline formations were not detected. In the three aortas, no isolated cholesterol crystals were found without adjacent calcium phosphate.

A multilayered particle, about 17 μm long, is positioned at the center of the SEI photomicrograph in Fig. 5a. It is comprised of smooth surfaced plates that have right angles on one side. The dark background was identified as apatite by EDX, with a spectrum similar to that shown in Fig. 1b. In Fig. 5b the CL image of this particle is shown, identifying it as a structure comprised of cholesterol plates. The contours in Figs. 5a and 5b match perfectly. Figs. 5c and 5d show calcium and phosphorus maps, respectively. The place occupied by the crystal identified in Fig. 5b as cholesterol is seen as a black space, which, according to the technique employed, indicates a complete absence of calcium and phosphorus in this area.

The integration of the SEM methods used in this study allowed us to distinguish clearly between the inorganic and the organic parts of the lesion structures. The SEI analysis showed the overall features (Figs. 1a, 1c, 3a, 4a, and 5a). The BSEI showed the contours of the mineral parts (Fig. 3b). The EDX identified the mineral parts as calcium phosphate, more precisely as apatite (Fig. 1b and determinations not shown). Mapping of the elements Ca and P delineated and co-localized these mineral lesion components (compare Figs. 4b with 4c and 4d). The organic parts were delineated by their negative responses to EDX (Fig. 1d), to BSEI (Fig. 3b) and to element mapping (Figs. 4c, 4d, 5c, and 5d).

The parts that were determined as organic could be either cholesterol crystals or organic, non-crystalline materials. SEI analysis gave a rough indication of the nature of the organic tissue parts. Normal tissue does not usually have crystalline forms. However, cholesterol can exist in lesions as plate-like crystals (Fig. 3a).

When viewed from above, these crystals have flat smooth faces with well shaped angles (Fig. 5a). To confirm that these structures were cholesterol crystals, we employed CL to distinguish between other tissue elements and cholesterol crystals. It is known that compounds possessing five and six membered rings yield much stronger CL signals than compounds which contain only linear bonds (Giles, 1975). As most organic tissue materials do not contain several aromatic rings in one molecule, we expected to find an enhanced CL signal only from a cholesterol crystal, due to the dense aromatic ring structure. Such signals were demonstrated in Figs. 2, 3c and 5b. Only a faint CL response was emitted from the non-crystalline, organic area visualized in Fig. 1c (data not shown). Thus, it may be concluded that the integration of all the employed techniques identifies the mineral and crystalline cholesterol parts of the lesions.

The finding of this study is that apatite and cholesterol crystals (several micrometers to a few tens of micrometers in size) form closely linked agglomerates, several tens or hundreds of micrometers in size, in which the crystals are very close. The relative positions of the calcium phosphate and cholesterol crystals are rather haphazard and unaligned. Moreover, the agglomerates form an irregular pattern in the lesion tissue. These findings suggest the intriguing question as to whether the precipitation of one kind of crystal (i.e., cholesterol or calcium phosphate) in a specific location may trigger the precipitation of the other kind of crystal, that would otherwise remain solubilized. Although we have not found direct evidence of epitaxial growth of calcium phosphate on cholesterol crystals or the reverse, it cannot be concluded that this does not occur. Further studies are needed to study this possibility and to determine if precipitation of cholesterol and calcium are indeed linked during the atherosclerotic disease process.

Acknowledgements

We wish to thank the United States-Israel Binational Science Foundation for financing this study; Mr. Michael Dvorachek for his highly professional and devoted performance of the SEM determinations; Dr. Sorin Katz for introducing us to the cathodoluminescence technique; and Carol Kosh for expert secretarial assistance.

References

Bittman R, Fischkoff SA (1972). Fluorescence studies of the binding of the polyene antibiotics filipin III, amphotericin B, nystatin and lagosin to cholesterol. Proc Natl Acad Sci USA **69**: 3795-3799.

Boyde A, Maconnachie E, Reid SA, Delling G, Mundy GR (1986). Scanning electron microscopy in bone pathology: Review of methods, potential and applications. Scanning Electron Microsc **1986**;IV: 1537-1554.

deKruijff B, Demel RA (1974). Polyene antibiotic-sterol interactions in membranes of *Acholeplasma Laidllawii* cells and lecithin liposomes. III. Molecular structure of the polyene antibiotic-cholesterol complexes. Biochim Biophys Acta **339**: 57-70.

Giles PL (1975). Cathodoluminescence. J Microscopie Biol Cell **22**: 357-370.

Hirsch D, Azoury R, Sarig S (1990). Co-crystallization of cholesterol and calcium phosphate as related to atherosclerosis. J Crystal Growth **104**: 759-765.

Hollander W (1976). Unified concept on the role of acid mucopolysaccharides and connective tissue proteins in the accumulation of lipids, lipoproteins and calcium in the atherosclerotic plaque. Exp Mol Pathol **25**: 106-120.

Kruth HS (1984). Localization of unesterified cholesterol in human atherosclerotic lesions. Demonstration of filipin-positive, oil red-0 negative particles. Am J Pathol **114**: 201-208.

Lerner E, Azoury R, Sarig S (1989). Rapid precipitation of apatite form ethanol-water solutions. J Crystal Growth **97**: 725-730.

Matonoha P, Zechmeister A (1978). Scanning electron microscopic observation of intimal surface of normal and atherosclerotic arteries. Acta Morphologica Acad Sci Hung **26**: 173-184.

Meyer WW (1977). The mode of calcification in atherosclerotic lesions. Adv Exp Med Biol **82**: 786-792.

Norman AW, Demel RA, deKruyff B, van Deenen LLM (1972). Studies on the biological properties of polyene antibiotics: Evidence for the direct interaction of filipin with cholesterol. J Biol Chem **247**: 1918-1929.

Pease RFW, Hayes TL (1966). Scanning electron microscopy of biological material. Nature **210**: 1049.

Schmid K, McSharry WO, Pameijer CH, Binette JP (1980). Chemical and physicochemical studies on the mineral deposits of the human atherosclerotic aorta. Atherosclerosis **37**: 199-210.

Sims FH (1989). A comparison of structural features of the walls of coronary arteries from 10 different species. Pathology **21**: 115-124.

Tanimura A, McGregor DH, Anderson HC (1986). Calcification in atherosclerosis. 1. Human Studies. J Exp Pathol **2**: 261-273.

Tomazic BB, Brown WE, Queral LA, Sadovnik M (1988) Physicochemical characterization of cardiovascular calcified deposits. Atherosclerosis **69**: 5-19.

Discussion with Reviewers

B.B. Tomazic: The reported EDX Ca/P ratio was about 5:3. What kind of ratio variation was established? The EDX data on the Ca/P ratio obtained in another study (Tomazic *et al.*, 1988) indicates the variability of the ratio showing the heterogeneity of bioapatites. Did the present study show a similar trend?

H. Harasaki: The authors conclude, prematurely that calcium phosphate detected in atherosclerotic lesions by EDX is apatite, because the Ca:P molar ratio is 5:3. Although the authors state that calibrated standards were used to identify Ca and P, no quantitative data have been provided to support the above-mentioned ratio of 5:3.

It is not clear whether the ratio was always 5:3, when Ca and P were detected. With anhydrous preparation, amorphous calcium phosphate, which does not necessarily have a molar ratio of 5:3, may be preserved without translocation as precursors to a crystalline form. Other crystalline calcium phosphates, such as octacalcium phosphate with a molar ratio of 4:3, may exist as precursors to hydroxyapatite (Tomazic *et al.*, 1988). In dystrophic calcification, such as calcification seen in atherosclerotic lesions, calcium phosphate may not always be pure apatite, but agglomerate of calcium phosphates of various molar ratios and a mixture of crystalline and amorphous forms. Please comment.

A.L. Boskey: Even with numerous standards, there is great uncertainty in EDX analysis of Ca and P. More importantly, **Ca:P ratio cannot be used to identify phases**. Synthetic apatites can be prepared with surface adsorbed phosphates, such that Ca:P molar ratio is close to 1:1, or as high as 2:1. Although numerous studies have identified the mineral in the lesions as apatitic, there have been reports of octacalcium phosphate in these lesions. A Ca:P ratio close to 5:3 can be found for amorphous tricalcium phosphate $Ca(PO_4)_6$, octacalcium phosphate $Ca_8H_2(PO_4)_6$, or apatite $Ca_{10}(PO_4)_6(OH)_2$, especially when phosphoproteins are adsorbed on the surface, yielding lower values than expected for the mineral phase present. X-ray or electron diffraction evidence of the apatitic nature of the lesion should be cited. From the colored Figure, it appears that at any given site, ratios are 10:4 or 10:5 and not 10:6.

Authors: As stated in the text, the crystalline structures that were examined in detail (and presented in the manuscript) were selected based on their having a 5:3 Ca:P ratio characteristic of apatite. A visual estimate of the ratio from the EDX scan was first made. For regions that were further examined, a ratio of 5:3 was confirmed by calculation (this includes the mineral deposit demonstrated in the color Figure 4 referred to by Dr. Boskey). However, not all regions in which a 5:3 ratio was apparent by visual inspection of the EDX scan were studied in detail. Even though calculations were not made for these areas, we do not believe that they would have varied by more than $\pm 5\%$. There were other mineral-containing regions that had other than 5:3 ratios by visual inspection, but these areas were not examined in this study. It was not our intent nor can we estimate the variation in these other areas. To repeat, as stated in the manuscript: "we studied only those mineral deposits with a 5:3 Ca:P molar ratio, characteristic of apatite".

B.B. Tomazic: Is it possible to produce quantitative assessment of the cholesterol:apatite ratio, or, alternatively, of the cholesterol:Ca:P ratio in aortic tissue using the combined SEM techniques and in this way supplement and challenge the results of classical chemical analyses used by Fleckenstein *et al.* [Fleckenstein A, Frey M, Thimm F, Fleckenstein-Grün (1990) Excessive mural calcium overload - A predominant casual factor in the development of stenosing coronary plaques in humans. Cardiovascular Drugs and Therapy **4**: 1005-1014]? Figures 5c and 5d appear different in the apparent presence of some phosphorous in the black field corresponding to cholesterol. Is that a fact or the imaging error? Is it possible to ascertain the threshold level of detection of the inorganic matrix in a cholesterol crystal? This information would be very useful in attempting to establish a possible link between cholesterol and calcium during the progression of the atherosclerotic condition.

Authors: We do not know whether the signals obtained from the various SEM techniques could be used to accurately quantify cholesterol and apatite constituents in lesions or other tissues. Future work with these techniques is necessary to establish the threshold as well as the linearity of response of these techniques for cholesterol and apatite detection.

A.L. Boskey: Is there any solution data suggesting that cholesterol crystals can support apatite nucleation and/or growth, or vice versa?

Authors: We are not aware of such data. However, Craven (Nature 1976, **260**: 727-729) has suggested that because of similarities in crystal structure of hydroxyapatite and cholesterol monohydrate, a microcrystal of either may serve as a nucleus for the growth of the other.

A.L. Boskey: Were plaque-free sites sampled? If not, how can the authors conclude cholesterol is not seen without coexisting mineral crystals? Perhaps in less diseased areas mineral is present without cholesterol or vice versa.

Authors: In the present limited study of advanced lesions from 3 aortas, cholesterol crystals and mineral were in close proximity. However, we do not know whether this would be seen in earlier stages of lesion development. It will be of interest to apply the described techniques to address this question.

D.C. Morris: Did you compare the appearance of extracted lesions versus non-extracted lesions. Given the possibility that there may be some cell debris associated with the agglomerates, how much of the cathodoluminescence is due to the cholesterols and perhaps, proteinaceous debris?

Authors: Other non-crystalline areas showed much lower levels of cathodoluminescence compared to the crystal structures.

D.C. Morris: Transmission electron micrographs of Nanoplast-embedded agglomerates would offer a corresponding sub-cellular image of these structures; have the authors tried any non-solvent TEM processing to look at ultrastructural detail?

Authors: We have not carried out these types of experiments at this point.

D.C. Morris: Have the authors examined any of the experimental models of atherosclerosis to determine how and where agglomerate formation might be initiated?

Authors: Although it may be difficult to reproduce in animal models those mechanisms of calcification that occur in human atherosclerotic lesions, we plan to carry out such experiments in the future.